Environmental Nanotechnology, Monitoring & Management 14 (2020) 100312

Contents lists available at ScienceDirect

Environmental Nanotechnology, Monitoring & Management

journal homepage: www.elsevier.com/locate/enmm

Mycosynthesis of gold nanoparticles by the Portabello mushroom extract, Agaricaceae, and their efficacy for decolorization of Azo dye

Mohammed Ali Dheyab[a], Mustafa Nadhim Owaid[b,c,*], Muwafaq Ayesh Rabeea[d], Azlan Abdul Aziz[a], Mahmood S. Jameel[a]

[a] Nano-Optoelectronics Research and Technology Lab (NORLab), School of Physics, Universiti Sains Malaysia, 11800 Pulau Pinang, Malaysia
[b] Department of Heet Education, General Directorate of Education in Anbar, Ministry of Education, Hit, 31007 Anbar, Iraq
[c] Department of Environmental Sciences, College of Applied Sciences-Hit, University Of Anbar, Hit, 31007 Anbar, Iraq
[d] Department of Applied Chemistry, College of Applied Sciences-Hit, University Of Anbar, Hit, 31007 Anbar, Iraq

ARTICLE INFO

Keywords:
Agaricus bisporus
AuNPs
Fungi
Mycosynthesis
Textile dye

ABSTRACT

This research is the first attempt on using fruitbodies of Portabello mushroom (*Agaricus bisporus*) as a newly mycoreducer agent used in the myco-synthesis of gold nanoparticles (AuNPs). The biosynthesized AuNPs were described for their chemical and physical characteristics by UV–vis spectra, the change in color, AFM, FESEM, XRD, Zeta Potential, DLS, and FT-IR analyses. The AuNP was investigated for its activity to decolorize MB (Methylene Blue) dye. However, the magenta color of gold nanoparticles indicated that the colloidal AuNPs contained a mixture of oval, spherical, drum-like, hexagonal, and triangular shapes reaches 53 nm in the diameter. Clearly, XRD exhibited that the formed Au nanoparticles in this study were crystalline. In contrast, data of Zeta Potential and DLS exhibited that myco-synthesized gold NPs showed remarkable aggregation and stability characteristics in the colloidal AuNPs solution. FTIR revealed the attachment of the amino acid, polysaccharide, and phenol as a mycoreducer agent capped gold NPs. The degradation activity showed that decolorizing Methylene Blue increased with the increasing the time of incubation in the finding of gold NPs. The myco-synthesized AuNPs using extracts of *Agaricus bisporus* can act as nanocatalysts in the reduction of Methylene Blue which showed the best decolorization at 97.98%.

1. Introduction

The Myconanotechnology is a term given to the green synthesis of metallic and non-metallic nanoparticles from several organic myco-materials present in the fungus such as yeast, mold, and mushroom (Owaid et al., 2019a; Owaid and Ibraheem, 2017). In different researches, the nanoparticle was formed by chemical routes by different reducing agents, but these routes might be damaged human health when they are employed in many biomedical applications or to reduce most organic pollutants in nature (Noruzi et al., 2011; Shang et al., 2013). Lately, the bio-synthesis of nanoparticles using ecofriendly methods is utilized to decrease the cytotoxicity of chemicals by using different biological materials (Virkutyte and Varma, 2011) isolated from the alga (Kathiraven et al., 2015), plant (Al-Bahrani et al., 2018; Noruzi, 2015; Owaid et al., 2019b), mushroom (Owaid, 2019; Owaid et al., 2015) and truffle (Owaid et al., 2018a,b,c).

This method is known the green method or green chemistry used to synthesize NPs, which considered eco-friendly. Indeed, usage of macrofungi in the mycosynthesis of various metallic and non-metallic nanoparticles is too useful because of producing huge amounts of fruitbodies, mycelia, and enzymes, worldwide (Owaid and Ibraheem, 2017). The biosynthesis of different shapes of nanoparticles like triangular is more complicated than other shapes (Sun et al., 2003). However, only few studies have succeeded to biosynthesize spherical and triangular gold NPs (Owaid, 2019) from the edible mushrooms, including *Flammulina velutipes* (Rabeea et al., 2020) *Lentinula edodes* (Owaid et al., 2019a), *Pleurotus sapidus* (15 – 100 nm) (Sarkar et al., 2013), *Pleurotus florida* (10 – 50 nm) (Bhat et al., 2013), and *Volvariella volvacea* (20 – 150 nm) (Philip, 2009). On the other hand, extracts of the *Agaricus bisporus* white strain were employed coupled with the method of microwave irradiation, to mycosynthesize just the gold NPs sphere with 20 nm (diameter) (Eskandari-Nojedehi et al., 2018) and 50 nm (Eskandari-Nojehdehi et al., 2016). The mycosynthesized AgNPs from *A. bisporus* white strain have antibacterial (Narasimha et al., 2011; Pipriya and Tiwari, 2019; Sujatha et al., 2013) and antifungal activity (Sudhakar et al., 2014), while the AuNPs synthesized from *A. bisporus*

* Corresponding author.
E-mail addresses: mustafanowaid@uoanbar.edu.iq, mustafanowaid@gmail.com (M.N. Owaid).

https://doi.org/10.1016/j.enmm.2020.100312
Received 15 April 2020; Received in revised form 3 May 2020; Accepted 13 May 2020

white strain have antibacterial (Eskandari-Nojehdehi et al., 2016) and antifungal activity (Eskandari-Nojedehi et al., 2018).

Recently, some recent studies have reported that AuNPs synthesized using extracts of molds (Qu et al., 2017) and plants (Rodríguez-León et al., 2019) may be used for catalytic activity evaluations in the degrading the organic dye used in industry fields. Only few studies have also emerged that the biosynthesized AgNPs from the mushroom showed catalytic activity toward Azo dyes like the oyster mushrooms species *Pleurotus ostreatus* (Karthikeyan et al., 2019) and *P. sajor caju* (Nithya and Ragunathan, 2009). However, only one study (Rabeea et al., 2020) has been published showed using mycosynthesized AuNPs from *Flammulina velutipes* to degrade the MB dye.

Agaricus bisporus is a healthy fresh food (Atila et al., 2017) cultivated on organic substrates (Owaid et al., 2018a,b,c; Rashid et al., 2018) and grown naturally in Iraq and worldwide (Owaid et al., 2018a,b,c). Recently, it is important to synthesis of green silver nanoparticles (Owaid et al., 2017b). Just for the first time, *Agaricus bisporus* white strain was used to mycosynthesize spherical Au nanoparticles with sizes ranging from 10 − 50 nm (Eskandari-Nojedehi et al., 2018; Eskandari-Nojehdehi et al., 2016), but no published researches were ever performed in the gold NPs synthesis from the extract of fruit bodies of *Agaricus bisporus* brown strain. Thus, this work is considering the first try for the extracellular myco-synthesizing spherical, oval, drum-like, triangular, and hexagonal gold NPs using fruitbodies of brown button mushroom (Portabello) *Agaricus bisporus*. Also, the biosynthesized AuNPs by *Agaricus bisporus* were investigated for degradation of MB (methylene blue) dye as a first try from NPs mycosynthesized from this mushroom.

2. Materials and methods

2.1. PortabelloMushroom samples

Fresh *Agaricus bisporus* (Portabello mushroom) fruitbodies (150 g) were obtained from the supermarket which cultivated at Champ Fungi Sdn. Bhd., Port Klang, Malaysia.

2.2. Portabellomushroom extraction

The fresh Portabello mushroom watery extract was performed by taking twenty grams of this mushroom, which cut, extracted in a 250 mL flask with hundred fifty milliliters of D.W (distilled water), and boiled until the tenth minute. The extracted crude solution was placed to cool down to 25 °C. Nevertheless, the mushroom extract was filtered using gauze and the filter paper and centrifuged at 6000 rpm for 10 min. The final watery extract was saved at − 20 °C until use (Owaid et al., 2019a).

2.3. The myco-fabrication of gold nanoparticles

The following route performed the mycological fabrication of AuNPs. Briefly, 135 mL of 1×10^{-3} M solution of Chloroauric acid ($HAuCl_4.4H_2O$, Sigma Aldrich, Germany) was heated on the magnetic stirrer from 80 to 100 °C in a 250-ml flask. After that, about 15 mL of *A. bisporus* (Portabello mushroom) aqueous extract was mixed with the solution of Chloroauric acid. The color of the interaction mixture changed to light magenta after 30 min, and the process continued to 90 min until the constancy of the color of mixture to deep purple color. The change in color indicated the formation of AuNPs, which proven by UV–vis spectra (Owaid et al., 2019a).

2.4. Characterizing AuNPs

The mycosynthesized AuNPs from the *Agaricus bisporus* extract were characterized by UV–vis spectra, the change in color, FTIR, FE-SEM, Dynamic Light Scattering (Zetasizer Nano ZS), XRD, AFM, and Zeta Potential analyses. All these tests were performed in Malaysia at Universiti Sains Malaysia (USM).

2.5. Methylene blue decolorization

The fabricated AuNPs were used to nano-degrade the dye of MB (methylene blue, 10 ppm). Only 1 mg of NPs was used to decolorize 10 mL MB (10 ppm) by shaking for 5, 10, and 15 min on the magnetic stirrer at 25 °C. To evaluate the MB decolorization by AuNPs, the lambda max at 670 nm was performed using UV–vis, and the percentage was determined using the following equation (Jyoti and Singh, 2016):

$$\text{Decolorization of methylene blue, } \% = \frac{M_0 - M}{M} * 100$$

Where M_0 is the initial concentration of MB dye, M is the concentration after degradation of MB by AuNPs.

3. Results and discussion

The extracellular reducing Au° using the mycoreducting Au^{+} ions by Portabello mushroom *Agaricus bisporus* fruit bodies haven't been investigated formerly. Fig. 1 exhibits that the color of the *A. bisporus* extract mixed with the 0.001 M $HAuCl_4.4H_2O$ has changed from light yellow to magenta. The present color is considered as an indicator to successful mycosynthesis of AuNPs in this study, which agreed with the visual vision of AuNPs from another study (Owaid et al., 2017a) who mycosynthesized AuNPs using the *Pleurotus cornucopiae,* oyster mushroom. In the current study, 5 periods were used to biosynthesize these NPs from the *A. bisporus* fruiting body, viz. 30 min, 45 min, 60 min, 75 min, and 90 min at 80 °C using a magnetic stirrer hotplate. Nevertheless, the interaction mixture changed to bright magenta after 30 min, which referred to the primary formation of gold NPs. Also, the intensity of color increased with increasing the interaction time, which indicated that the biosynthesis of more gold NPs, see Fig. 1. The visual test increased with increasing the reaction time too, and mycocompounds reduced more Au + in the reaction mixture (Owaid et al., 2017a). In fact, the AuNPs intensity relates with the concentration of proteins, and polysaccharides, which reduced and capped the present nanomaterials, as mentioned by many last studies (Philip, 2009).

The UV–vis spectrum of gold NPs from 400 nm to 700 nm and the lambda max at 559 nm were noticed due to the Surface Plasmon Resonance incitation in the colloidal AuNPs. The UV–vis spectrum exhibits a variation in the lambda max according to increasing of the reaction time. As seen in Fig. 1, the lambda max of colloidal gold nanoparticles redshifted from 557 − 559 nm at 30 − 90 min. At 30 min, the biggest intensity absorbance was 1.019 a.u.; afterward, the absorbance increased to 1.229, 1.371, and 1.476 a.u. after 45, 60, and 75 min from the reaction time for the wavelength of 559, 558, and 558 nm. However, at 90 min, AuNPs exhibited the bigger absorbance reached 1.615 cm^{-1} at 558 nm in this study. Thus, the venatic relation between the absorbance wavelength and the increasing color intensity was clear. The UV–vis spectrum supported the phenomenon of SPR discovers for gold (Singh et al., 2016). It is observed from the UV–vis spectrum that the AuNP peak occurred at 558 nanometers, and the last adsorption steadily increased with the increase of the time of reaction. However, the broadening, splitting, and red-shift of SPR are probable because of the dampening of SPR phenomenon created by the alteration in the refractive index of the surrounding environment and the increasing in sizes of AuNPs in the colloid (Basavaraja et al., 2008).

Fig. 2 exhibited the shapes and sizes of the synthesized AuNPs using *Agaricus bisporus*. Most of bio-synthesized AuNPs had spherical, oval, drum-like, hexagonal, and triangular shapes, see FESEM (Fig. 2). Nevertheless, the range of sizes was from 121.00 nm to 27.68 nm, as shown in Fig. 2. Differently, the AFM (Fig. 3) and the granularity histogram exhibited the distribution of AuNPs sizes average (53.0 nm), as

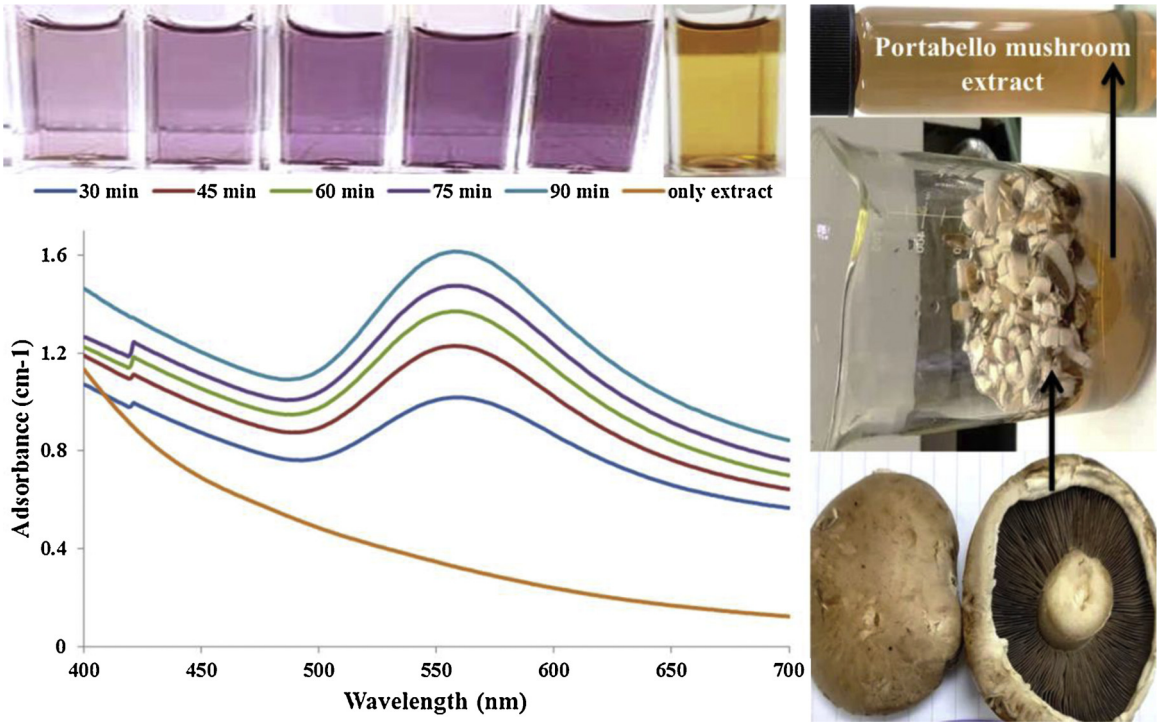

Fig. 1. The visual test and UV–vis spectra of gold NPs.

seen in Fig. 4.

The peaks of XRD in Fig. 5 located at 2θ of 77.55°, 64.56°, 44.38°, and 38.18° could be assigned to the crystallographic planes of 311, 220, 200, and 111, respectively for face-centered cubic Au crystals, that agrees with (Eskandari-Nojedehi et al., 2018), and corresponds with values of Ref. Code 01−089-3697 (Abod et al., 2017; Ghareib et al., 2016). The size averages of Au particles are 51.98, 53.05, 33.29, and 13.53 nanometers, respectively. The bigger intensity of 100% was recorded by the peak of 111, confirming that the current peak was a notable orientation, which exhibited the rate crystallite size of AuNPs was 51.98 nanometers. Evidently, the XRD pattern revealed that the nature of the biosynthesized AuNP was crystalline. The grains size average of AuNPs can be measured using Debye–Scherrer equation (Abdelrahim et al., 2017):

$$D = k.\lambda/\beta \cos \theta$$

Where D is the average thickness of crystal AuNPs vertically at the crystal plane (nm), θ is the diffraction angle, K is the constant of Scherrer (0.890), β is the FWHM (Full-Width Half Maximum), and λ (lambda) is the X-ray wavelength (CuK_{α} source) of 0.154 nanometers. The previous peaks recorded intensity percentages 100.0%, 45.4%, 23.9, and 24.0% at 2θ = 38.18°, 44.38°, 64.56°, and 77.55°, respectively which seen in Fig. 5.

Fig. 6A showed a standard FT-IR profile of the extract of *A. bisporus* to be employed as a reference profile. However, the band 3349 cm^{-1} relates to stretching vibrations of O—H in carbohydrate pattern (glucose and mannitol), whereas the aliphatic C–H stretching is recorded to a weak band near 2944 cm^{-1} (Xiang et al., 2016). The two minor bands 2894 cm^{-1} and 2794 cm^{-1} indicated to the stretch f O—H in the carboxylic acid and the phenolic compound. In contrast, the band 1638 cm^{-1} belonged to the carbonyl group of amide-I belonging to the peptide and C—N stretch of amino acid residue (Eskandari-Nojedehi et al., 2018). The band at 1404 cm^{-1} is the N—H stretching mode of the amine group in amino acids The band 1202 cm^{-1} and 1281 cm^{-1} may be associated to the C–H group in polysaccharides or to stretching vibration of phenol (C—O) or to a notable absorbance band for the lipid. Lastly, the band 1036 cm^{-1} may be associated to the beta D-linked glucopyranoside (Li et al., 2012) or the stretching C—O groups in the polysaccharide and the C—O—C group in the glucopyranose (Radzki and Kalbarczyk, 2010).

Fig. 6B revealed the bands of biosynthesized gold NPs by *A. bisporus* (Portabello mushroom). The band of 3358 cm^{-1} revealed the presence

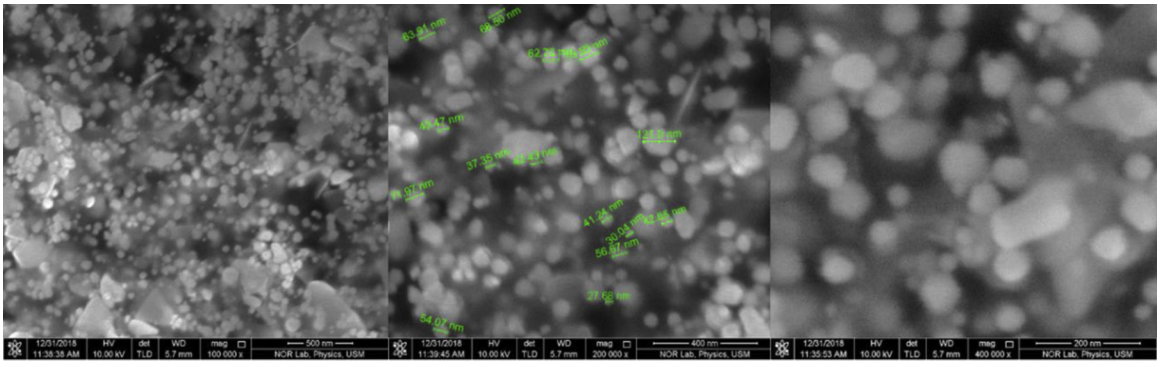

Fig. 2. FESEM of myco-synthesized AuNPs.

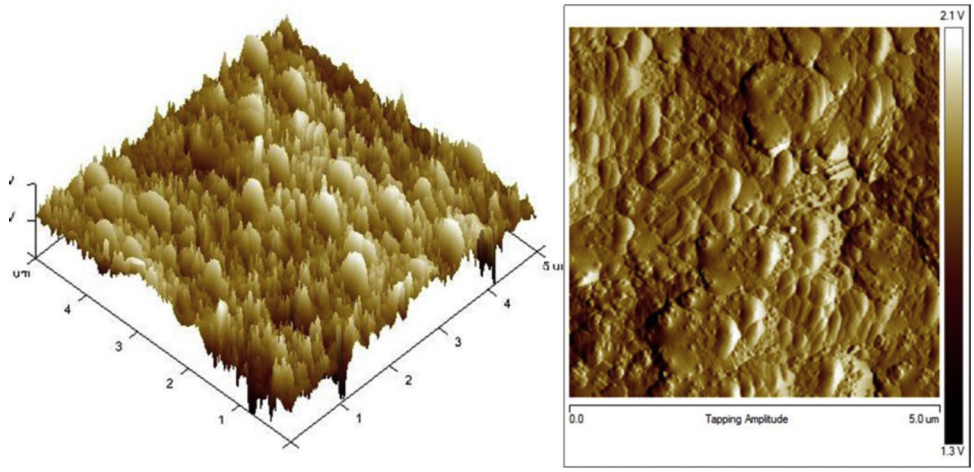

Fig. 3. 2D and 3D images of AFM of the biosynthesized AuNPs.

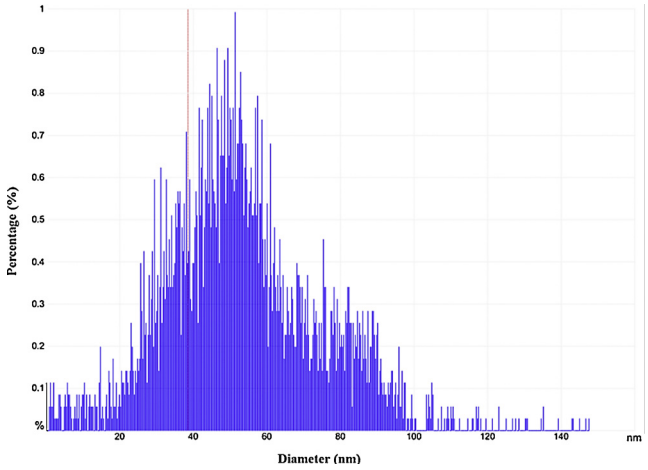

Fig. 4. The histogram of granularity of biosynthesized AuNPs.

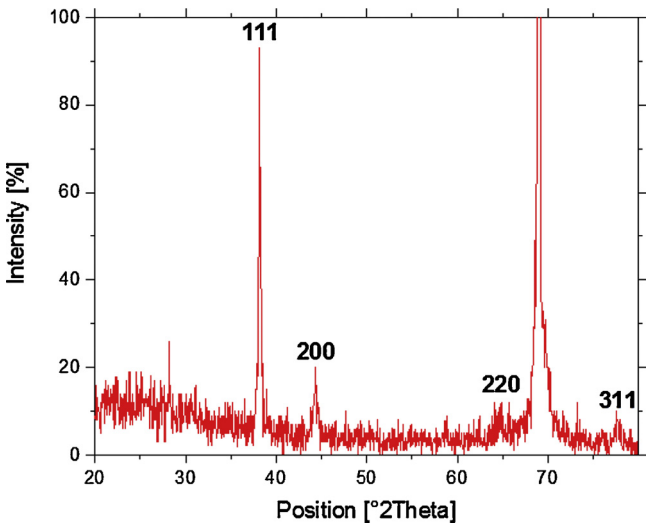

Fig. 5. XRD of myco-synthesized AuNPs from the *A. bisporus* extract.

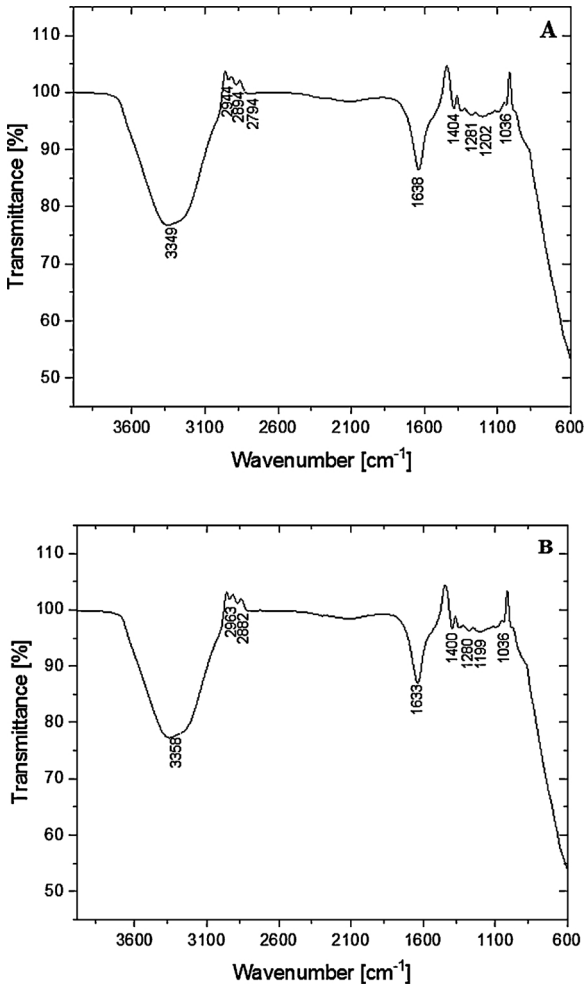

Fig. 6. FT-IR of the *A. bisporus* extract (A) and the green synthesized AuNPs (B).

of stretching vibrations in the hydroxyl (O—H) group in sugars. Moreover, the last group found in the two bands of 1199 and 1280 cm^{-1} (Socrates, 2004). The bands 2963 and 2882 cm^{-1} reverted to the stretching —CH. Also, the C—N stretch of amide I in the protein attributed to the band 1633 cm^{-1} as in FTIR of the *A. bisporus* extract (Fig. 6A). The band 1036 cm^{-1} associated with the group of C—O—C in carbohydrates (exactly in the glucopyranose), while the band 898 cm^{-1} associated with the aromatic structures (—CH). The band at 1400 cm^{-1} associated with the presence of stretch the group of R—COOH in the carboxylic acid (Li et al., 2012).

The stability of myco-synthesized gold NPs was investigated using the zeta potential calculation, as in Fig. 7. Nevertheless, it showed surface zeta potential, which revealed the charge of the surface on gold NPs. Also, the zeta potential value exhibited the constancy of the myco-

Results

		Mean (mV)	Area (%)	St Dev (mV)
Zeta Potential (mV): -2.26	Peak 1:	-2.26	100.0	8.30
Zeta Deviation (mV): 8.30	Peak 2:	0.00	0.0	0.00
Conductivity (mS/cm): 1.43	Peak 3:	0.00	0.0	0.00
Result quality : Good				

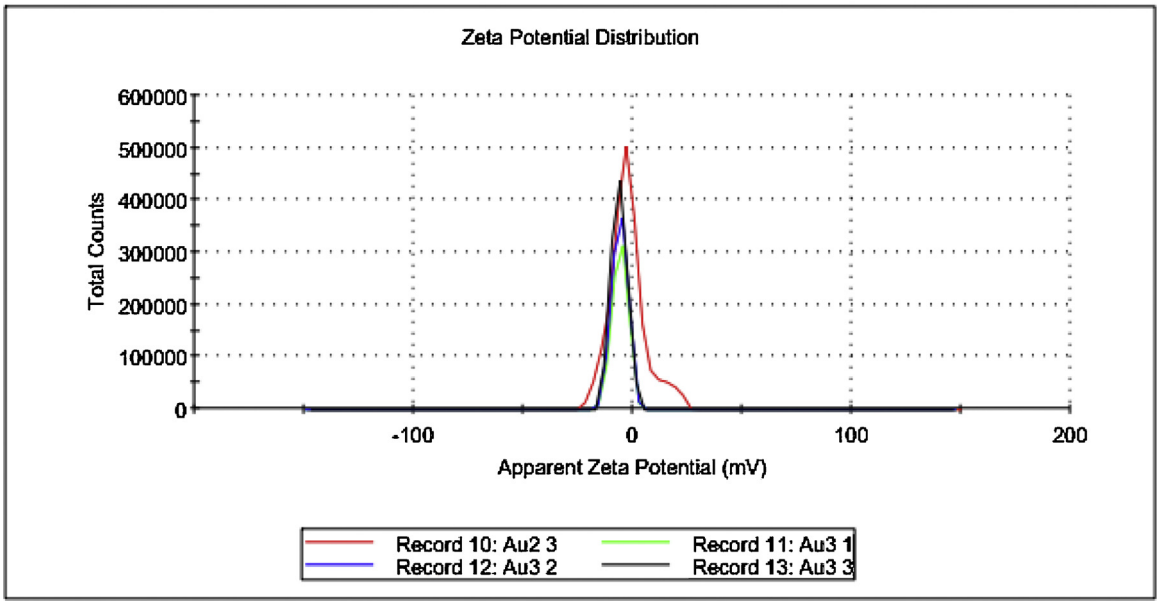

Fig. 7. The distribution of Zeta potential of myco-synthesized gold NPs.

synthesized nanoparticle (Srikar et al., 2016). Hence, the myco-synthesized gold NPs showed a good value for zeta potential reached -2.26 ± 8.30 mV formed from the Portabello mushroom extract. Nevertheless, the zeta potential value referred to good quality with the Au nanoparticles aggregation. Nevertheless, the negative value of this measurement referred to that gold NPs are surrounded by organic compounds with negative charges, which reduce the repulsion of AuNPs and thus increase their stability (Suresh et al., 2011).

Numerous documented works have explained how the surface-active biomolecules (as stabilizers) produced electrostatic interactions in the interaction solution yield more stable AuNPs (Ahmad et al., 2015; Anand et al., 2015). It is suggested that mycoorganic molecules like proteins, amino acids, glycosides, alkaloids, flavonoids, and phenols may serve as stabilizers responsible for AuNPs mycosynthesis and constancy. If the potential surface value of NPs is from −30 mV to +30 mV, they become stable (Anand et al., 2015). In this work, the stable dispersions of gold NPs are definite, as shown in Fig. 7 (Zeta potential of -2.26 ± 8.3 mV).

The chemical reaction of organic molecules with gold ions by these natural mycomaterials leads to a reduction of the last (Au^{+}) and the forming the atom of Au (Au°) (Owaid and Ibraheem, 2017). The organic compounds in Portabello mushroom that interact with ions of Au to form Au atoms covered with amino acids, polysaccharides, and phenols, is definite in FTIR spectra of AuNPs (Figs. 6A & B) in this test.

By observing MB (methylene blue) dye decolorization, the catalytic efficacy of the myco-synthesized AuNPs by *A. bisporus* was tested. At various times, Fig. 8 showed the percentage of MB degradation by these AuNPs. The catalytic degradation of MB was calculated by the declining absorbance band intensity at 670 nm.

In addition, the absorption band at 670 nanometers for MB dye, which progressively reduced with the increase in interaction time, demonstrates that this dye was slowly degrading, according to Reddy et al. (Reddy et al., 2015) findings. In comparison with the methylene

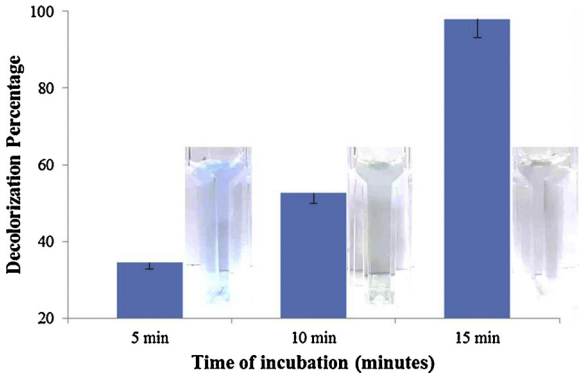

Fig. 8. Methylene blue decolorization by myco-synthesized AuNPs.

blue alone that remained deep blue (control), colors in the mixed dye with the colloid of AuNPs progressively changed over time from deep blue to bright blue. In another phrase, the catalytic action of these *A. bisporus*-AuNPs exhibited degrading methylene blue to leuco-methylene blue, as in Fig. 8. Increased incubation time has led to an increase in the decoloration efficacy of the dye reached 34.45%, 52.63%, and 97.98% after 5 min, 10 min, and 15 min, respectively, as seen in Fig. 8.

These AuNPs, have high surface energy, play an influential role in reducing Azo dyes, where they serve as nanocatalysts effectively in the decoloring of methylene blue (Paul et al., 2015). Also, this is consistent with (Qu et al., 2017), who suggested that AuNPs can significantly increase the rate of organic dye decoloration with high catalytic ability.

The decoloring process of Methylene blue is attributed to natural compounds on the gold nanoparticle surfaces. Blue dye degradation did not happen in the absence of catalysts (AuNPs). MB carrying active group N═N is commonly used in fabrics and reduced to –NH–NH– (a colourless amine) by AuNPs, which used as nanocatalysts (Qu et al.,

2017). Mycosynthesized AuNPs also act as nanocatalysts in the redaction of this dye by bio-matters of *A. bisporus* found on the surface of AuNP. FT-IR (Fig. 6) revealed that active groups such as –NH, −COOH, and −OH could be reduced this specific dye. That is which suggested that the mechanism of adsorption was typically based on the chemical adsorption on the biomaterial surfaces of this mushroom around AuNPs through collaboration reaction, complexation, and electrostatic attraction, and agreed with (Wu et al., 2017).

4. Conclusion

The present work aimed to use *Agaricus bisporus* (Portabello mushroom) fruiting bodies to mycosynthesize the gold nanoparticle (AuNP) for the first time. These gold nanoparticles were described by UV–vis, the change in color, FT-IR, Zeta Potential, AFM, DLS, FE-SEM, EDX, and XRD analyses. The UV–vis spectrum revealed the lambda max at 568 nanometers because of the excitement of SPR in the colloidal solution of gold NPs. FT-IR spectra revealed the attachment of polysaccharides, amino acids, and phenols as green mycoreducer agents capped AuNPs. However, the magenta color of gold NPs indicated that the colloidal AuNPs contained a mixture of oval, spherical, drum-like, hexagonal, and triangular shapes reaches 53 nm in the diameter. The EDX indicates that the nanoparticle is AuNP. Clearly, the XRD pattern exhibited that mycosynthesized gold NPs in the current research were nanocrystalline. These nanoparticles exhibited the best MB degradation of 97.98% after 15 min. The MB degradation increased with the increasing time of incubation with gold nanoparticles. Finally, the biosynthesized gold nanoparticles using mycoorganic matters of *Agaricus bisporus* were active as nanocatalysts to reduce the dye of MB.

Component of the research Author's number

substantial contribution to conception and designM N Owaid
substantial contribution to acquisition of dataM. A. Dheyab, M. S. Jameel
substantial contribution to analysis and interpretation of dataM A Rabeea, M. A. Dheyab
drafting the articleM N Owaid, M A Rabeea
critically revising the article for important intellectual contentA Abdul Aziz, M. S. Jameel
final approval of the version to be publishedA Abdul Aziz

Declaration of Competing Interest

None.

Acknowledgments

Authors are thanking USM (Universiti Sains Malaysia) and especially the School of Physics staff for achieving measurements of the electron microscope and the Universiti Sains Malaysia Bridging Grant Number 304.PFIZIK.6316530 for funding the current research.

References

Abdelrahim, K., Younis, S., Mohamed, A., Salmeen, K., Mustafa, A.E.M.A., Moussa, S., 2017. Extracellular biosynthesis of silver nanoparticles using *Rhizopus stolonifer*. Saudi J. Biol. Sci. 24, 208–216. https://doi.org/10.1016/j.sjbs.2016.02.025.

Abod, H.A., Bander, I., Zain-Al-Abddeen, S.S., 2017. The effect of silver nanoparticles prepared using *Aspergillus niger* in some pathogenic bacteria Aspergillus niger. Kirkuk Univ. J./Sci. Stud. 12, 1–16.

Ahmad, A., Wei, Y., Syed, F., Imran, M., Khan, Z.U.H., Tahir, K., Khan, A.U., Raza, M., Khan, Q., Yuan, Q., 2015. Size dependent catalytic activities of green synthesized gold nanoparticles and electro-catalytic oxidation of catechol on gold nanoparticles modified electrode. RSC Adv. 5, 99364–99377.

Al-Bahrani, R.M., Muayad, S., Majeed, A., Owaid, M.N., 2018. Phyto-fabrication, characteristics and anti-candidal effects of silver nanoparticles from leaves of *Ziziphus mauritiana* Lam. Acta Pharm. Sci. 56, 85–92. https://doi.org/10.23893/1307-2080.APS.05620.

Anand, K., Gengan, R.M., Phulukdaree, A., Chuturgoon, A., 2015. Agroforestry waste *Moringa oleifera* petals mediated green synthesis of gold nanoparticles and their anticancer and catalytic activity. J. Ind. Eng. Chem. 21, 1105–1111. https://doi.org/10.1016/j.jiec.2014.05.021.

Atila, F., Owaid, M.N., Shariati, M.A., 2017. The nutritional and medical benefits of *Agaricus bisporus*: a review. J. Microbiol. Biotechnol. Food Sci. 7, 281–286. https://doi.org/10.15414/jmbfs.2017/18.7.3.281-286.

Basavaraja, S., Balaji, S.D., Lagashetty, A., Rajasab, A.H., 2008. Extracellular biosynthesis of silver nanoparticles using the fungus *Fusarium semitectum*. Mater. Res. Bull. 43, 1164–1170. https://doi.org/10.1016/j.materresbull.2007.06.020.

Bhat, R., Sharanabasava, V.G., Deshpande, R., Shetti, U., Sanjeev, G., Venkataraman, A., 2013. Photo-bio-synthesis of irregular shaped functionalized gold nanoparticles using edible mushroom *Pleurotus florida* and its anticancer evaluation. J. Photochem. Photobiol. B, Biol. 125, 63–69. https://doi.org/10.1016/j.jphotobiol.2013.05.002.

Eskandari-Nojedehi, M., Jafarizadeh-Malmiri, H., Rahbar-Shahrouzi, J., 2018. Hydrothermal green synthesis of gold nanoparticles using mushroom (*Agaricus bisporus*) extract: physico-chemical characteristics and antifungal activity studies. Green Process Synth. 7, 38–47. https://doi.org/10.1515/gps-2017-0004.

Eskandari-Nojehdehi, M., Jafarizadeh-Malmiri, H., Rahbar-Shahrouzi, J., 2016. Optimization of processing parameters in green synthesis of gold nanoparticles using microwave and edible mushroom (*Agaricus bisporus*) extract and evaluation of their antibacterial activity. Nanotechnol. Rev. 5, 537–548. https://doi.org/10.1515/ntrev-2016-0064.

Ghareib, M., Abu, M., Mostafa, M., Abdallah, W.E., 2016. Rapid extracellular biosynthesis of silver nanoparticles by *Cunninghamella phaeospora* culture supernatant. Iran. J. Pharm. Res. 15, 915–924.

Jyoti, K., Singh, A., 2016. Green synthesis of nanostructured silver particles and their catalytic application in dye degradation. J. Genet. Eng. Biotechnol. 14, 311–317. https://doi.org/10.1016/j.jgeb.2016.09.005.

Karthikeyan, V., Ragunathan, R., Jesteena, J., Kabesh, K., 2019. Green synthesis of silver nanoparticles and application in dye decolorization by *Pleurotus ostreatus* (MH591763). Glob. J. Bio-Scie. Biotechnol. 8, 80–86.

Kathiraven, T., Sundaramanickam, A., Shanmugam, N., Balasubramanian, T., 2015. Green synthesis of silver nanoparticles using marine algae *Caulerpa racemosa* and their antibacterial activity against some human pathogens. Appl. Nanosci. 5, 499–504. https://doi.org/10.1007/s13204-014-0341-2.

Li, N., Li, L., Fang, J.C., Wong, J.H., Ng, T.B., Jiang, Y., Wang, C.R., Zhang, N.Y., Wen, T.Y., Qu, L.Y., Lv, P.Y., Zhao, R., Shi, B., Wang, Y.P., Wang, X.Y., Liu, F., 2012. Isolation and identification of a novel polysaccharide–peptide complex with antioxidant, anti-proliferative and hypoglycaemic activities from the abalone mushroom. Biosci. Rep. 32, 221–228. https://doi.org/10.1042/bsr20110012.

Narasimha, G., Praveen, B., Mallikarjuna, K., Raju, D., 2011. Mushrooms (*Agaricus bisporus*) mediated biosynthesis of sliver nanoparticles, characterization and their antimicrobial activity. Int. J. Nano Dimens. 2, 29–36.

Nithya, R., Ragunathan, R., 2009. Synthesis of silver nanoparticle using *Pleurotus sajor caju* and its antimicrobial study. Dig. J. Nanomater. Biostruct. 4, 623–629.

Noruzi, M., 2015. Biosynthesis of gold nanoparticles using plant extracts. Bioprocess Biosyst. Eng. 38, 1–14.

Noruzi, M., Zare, D., Khoshnevisan, K., Davoodi, D., 2011. Rapid green synthesis of gold nanoparticles using *Rosa hybrida* petal extract at room temperature. Spectrochim. Acta Part A Mol. Biomol. Spectrosc. 79, 1461–1465.

Owaid, M.N., 2019. Green synthesis of silver nanoparticles by *Pleurotus* (oyster mushroom) and their bioactivity: review. Environ. Nanotechnol. Monit. Manage. 12, 100256. https://doi.org/10.1016/j.enmm.2019.100256.

Owaid, M.N., Ibraheem, I.J., 2017. Mycosynthesis of nanoparticles using edible and medicinal mushrooms. Eur. J. Nanomed. 9, 5–23. https://doi.org/10.1515/ejnm-2016-0016.

Owaid, M.N., Raman, J., Lakshmanan, H., Al-Saeedi, S.S.S., Sabaratnam, V., Ali, I.A., 2015. Mycosynthesis of silver nanoparticles by *Pleurotus cornucopiae* var. *citrinopileatus* and its inhibitory effects against *Candida* sp. Mater. Lett. 153, 186–190. https://doi.org/10.1016/j.matlet.2015.04.023.

Owaid, M.N., Al-Saeedi, S.S.S., Abed, I.A., 2017a. Biosynthesis of gold nanoparticles using yellow oyster mushroom *Pleurotus cornucopiae* var. *citrinopileatus*. Environ. Nanotechnol. Monit. Manag. 8, 157–162. https://doi.org/10.1016/j.enmm.2017.07.004.

Owaid, M.N., Barish, A., Shariati, M.A., 2017b. Cultivation of *Agaricus bisporus* (button mushroom) and its usages in the biosynthesis of nanoparticles. Open Agric. 2, 537–543. https://doi.org/10.1515/opag-2017-0056.

Owaid, M.N., Muslat, M.M., Abed, I.A., 2018a. Mycodegradation of reed straw, *Phragmites australis*. Curr. Res. Environ. Appl. Mycol. 8, 290–297. https://doi.org/10.5943/cream/8/2/12.

Owaid, M.N., Muslim, R.F., Hamad, H.A., 2018b. Mycosynthesis of silver nanoparticles using *Terminia* sp. Desert truffle, Pezizaceae, and their antibacterial activity. Jordan J. Biol. Sci. 11, 401–405.

Owaid, M.N., Seephueak, P., Attallah, R.R., 2018c. Recording novel mushrooms in Heet district, Iraq. Songklanakarin J. Sci. Technol. 40, 367–369. https://doi.org/10.14456/sjst-psu.2018.58.

Owaid, M.N., Rabeea, M.A., Abdul Aziz, A., Jameel, M.S., Dheyab, M.A., 2019a. Mushroom-assisted synthesis of triangle gold nanoparticles using the aqueous extract of fresh *Lentinula edodes* (shiitake), Omphalotaceae. Environ. Nanotechnol. Monit. Manage. 12, 100270. https://doi.org/10.1016/j.enmm.2019.100270.

Owaid, M.N., Zaidan, T.A., Muslim, R.F., 2019b. Biosynthesis, characterization and cytotoxicity of zinc nanoparticles using*Panax ginseng* Roots, araliaceae. Acta Pharm. Sci. 57, 19–32. https://doi.org/10.23893/1307-2080.APS.05702.

Paul, B., Bhuyan, B., Purkayastha, D.D., Dey, M., 2015. Green synthesis of gold

nanoparticles using *Pogestemon benghalensis* (B) O. Ktz. Leaf extract and studies of their photocatalytic activity in degradation of methylene blue. Mater. Lett. 148, 37–40. https://doi.org/10.1016/j.matlet.2015.02.054.

Philip, D., 2009. Biosynthesis of Au, Ag and Au–Ag nanoparticles using edible mushroom extract. Spectrochim. Acta Part A Mol. Biomol. Spectrosc. 73, 374–381. https://doi.org/10.1016/j.saa.2009.02.037.

Pipriya, S., Tiwari, U., 2019. Evaluation of antibacterial potential & phytochemical screening by the medicinal plant of *Acorus calamus* & *agaricus bisporus* & their synthesis of herbal silver nanoparticles with different solvents. Int J Eng Res Technol 8, 158–169.

Qu, Y., Shen, W., Pei, X., Ma, F., You, S., Li, S., Wang, J., Zhou, J., 2017. Biosynthesis of gold nanoparticles by *Trichoderma* sp. WL-Go for azo dyes decolorization. J. Environ. Sci. 56, 79–86. https://doi.org/10.1016/j.jes.2016.09.007.

Rabeea, M.A., Owaid, M.N., Aziz, A.A., Jameel, M.S., Dheyab, M.A., 2020. Mycosynthesis of gold nanoparticles using the extract of *Flammulina velutipes*, Physalacriaceae, and their efficacy for decolorization of methylene blue. J. Environ. Chem. Eng. 103841. https://doi.org/10.1016/j.jece.2020.103841.

Radzki, W., Kalbarczyk, J., 2010. Water soluble polysaccharides content in three species of edible and medicinal mushrooms: *lentinula edodes*, *Pleurotus ostreatus*, *Agaricus blazei*. Herba Pol. 56, 31–38.

Rashid, H.M., Abed, I.A., Owaid, M.N., 2018. Effect of Sesbania sesban on cultivation of *Agaricus bisporus*, Basidiomycota, and properties of spent mushroom compost outcome. Open Agric. 3, 652–657. https://doi.org/10.1515/opag-2018-0068.

Reddy, B., Madhusudhan, G., Ramakrishna, A., 2015. Catalytic reduction of methylene blue and Congo red dyes using green synthesized gold nanoparticles capped by *Salmalia malabarica* gum. Int. Nano Lett. 5, 215–222. https://doi.org/10.1007/s40089-015-0158-3.

Rodríguez-León, E., Rodríguez-Vázquez, B.E., Martínez-Higuera, A., Rodríguez-Beas, C., Larios-Rodríguez, E., Navarro, R.E., López-Esparza, R., Iñiguez-Palomares, R.A., 2019. Synthesis of gold nanoparticles using *Mimosa tenuiflora* extract, assessments of cytotoxicity, cellular uptake, and catalysis. Nanoscale Res. Lett. 14, 334. https://doi.org/10.1186/s11671-019-3158-9.

Sarkar, J., Kalyan, S., Laskar, A., Chattopadhyay, D., Acharya, K., 2013. Bioreduction of chloroaurate ions to gold nanoparticles by culture filtrate of *Pleurotus sapidus* Quel. Mater. Lett. 92, 313–316. https://doi.org/10.1016/j.matlet.2012.10.130.

Shang, Y., Min, C., Hu, J., Wang, T., Liu, H., Hu, Y., 2013. Synthesis of gold nanoparticles by reduction of HAuCl 4 under UV irradiation. Solid State Sci. 15, 17–23.

Singh, P., Kim, Y., Yang, D., 2016. A strategic approach for rapid synthesis of gold and silver nanoparticles by *Panax ginseng* leaves. Artif Cell Nanomed. B 44, 1949–1957.

Socrates, G., 2004. Infrared and Raman Characterisitc Group Frequencies. John Wiley Sons, Ltd.

Srikar, S.K., Giri, D.D., Pal, D.B., Mishra, P.K., Upadhyay, S.N., 2016. Green synthesis of silver nanoparticles: a review. Green Sustain. Chem. 6, 34–56. https://doi.org/10.4236/gsc.2016.61004.

Sudhakar, T., Nanda, A., Babu, S.G., Janani, S., Evans, M.D., Markose, T.K., 2014. Synthesis of silver nanoparticles from edible mushroom and its antimicrobial activity against human pathogens. Int. J. Pharmtech. Res. 6, 1718–1723.

Sujatha, S., Tamilselvi, S., Subha, K., Panneerselvam, A., 2013. Studies on biosynthesis of silver nanoparticles using mushroom and its antibacterial activities. Int. J. Curr. Microbiol. App. Sci. 2, 605–614.

Sun, Y., Mayers, B., Xia, Y., 2003. Transformation of silver nanospheres into nanobelts and triangular nanoplates through a thermal process. Nano Lett. 3, 675–679.

Suresh, A.K., Doktycz, M.J., Wang, W., Moon, J.W., Gu, B., Meyer III, H.M., Hensley, D.K., Retterer, S.T., Allison, D.P., Phelps, T.J., 2011. Monodispersed Biocompatible Ag2S Nanoparticles: Facile Extracellular Bio-fabrication Using the Gamma-proteobacterium, S. Oneidensis. Oak Ridge National Laboratory (ORNL); Center for Nanophase Materials Sciences; High Temperature Materials Laboratory.

Virkutyte, J., Varma, R.S., 2011. Green synthesis of metal nanoparticles: biodegradable polymers and enzymes in stabilization and surface functionalization. Chem. Sci. 2, 837–846.

Wu, J., Xia, L., Zhu, Y., Zhao, J., Zhang, X., Zhao, S., Wang, X., Zhang, T., 2017. Biosorption of malachite green, Safranine t and methylene blue onto spent substrate of *Flammulina velutiper*. Mod. Environ. Sci. Eng. 3, 412–418. https://doi.org/10.15341/mese(2333-2581)/06.03.2017/006.

Xiang, Y., Jun, Q., Zhen, L., Yaning, L., Anlong, Z., Yingkun, S., 2016. Research on the infrared spectroscopy of spent mushroom compost. Nat. Environ. Pollut. Technol. 15, 701–705.